

Experimental Observation of the Shear Alfvén Resonance in a Tokamak

F. D. Witherspoon, S. C. Prager, and J. C. Sprott

Department of Physics, University of Wisconsin, Madison, Wisconsin 53705

(Received 18 May 1984)

Experiments in Tokapole II demonstrate the shear Alfvén resonance in a tokamak by direct probe measurement of the wave magnetic field within the plasma. The resonance is driven by external antennas and is identified as radially localized enhancements of the poloidal wave magnetic field. The radial location agrees with calculations which include toroidicity and noncircularity of the plasma cross section. Other properties such as polarization, radial width, rise time, and wave enhancement also agree with magnetohydrodynamical theory.

PACS numbers: 52.40.Db, 52.55.Gb

It is sometimes the case that the dispersion relation for propagating waves in a uniform plasma, such as electrostatic plasma waves¹ and shear Alfvén waves,² becomes a condition for a local resonance in a nonuniform plasma. Such resonances can be used to couple energy to the plasma from external sources. Although utilization of the shear Alfvén resonance for plasma heating was proposed more than ten years ago,^{3,4} experimental application to tokamaks has only just recently begun, at several institutions.⁵⁻⁹ Earlier experiments were carried out in a linear pinch¹⁰ and in stellarator devices.¹¹

The experimental base for shear Alfvén resonance heating is still in a very early stage of development, with much of the theory, including that pertaining to the properties of the resonance itself, not yet confirmed by experiment in tokamaks. The resonance has been observed in linear devices¹² and somewhat less directly in stellarators,¹¹ but not heretofore in a tokamak. Questions then arise as to whether the resonance actually exists in a tokamak with properties consistent with magnetohydrodynamical (MHD) theory, and whether energy can be coupled to the plasma through this resonance from external antennas. The resonance condition depends on the dimensionality of the system^{13,7} and differs in a two-dimensional (2D) tokamak from the simple 1D cylindrical criterion that the parallel phase speed match the local Alfvén speed. We have thus preceded high-power heating experiments with careful identification of the resonance in a tokamak at moderate power levels. We report here measurements of the properties of the resonance and a comparison with a 2D calculation by Kieras and Tataronis¹³ in which the ideal MHD equations are solved for the Tokapole II device, including both toroidicity and noncircularity of the plasma cross section.

The resonance is detected through the wave magnetic field inside the plasma. According to MHD theory, three perturbation quantities are associated

with the wave—the wave fluid velocity \vec{v} , magnetic field \vec{B} , and plasma pressure \tilde{p} . At the resonant location, where the drive frequency and mode structure of the antenna provides a match to the local Alfvén velocity, \vec{v} is predicted to be infinite but is not a readily measurable quantity. The perturbed pressure of the wave is a somewhat indirect indicator of the resonance. If the equilibrium plasma pressure is zero (a good approximation for this low-beta experiment), MHD implies that \tilde{p} is zero. If the equilibrium pressure is nonzero, \tilde{p} does become infinite at the resonance, but much more weakly than \vec{B} . At the resonance $\tilde{p}/\vec{B} \rightarrow 0$ even though \tilde{p} and \vec{B} both go to infinity. For the largest measured values of \vec{B} in these experiments, $\tilde{p}/p < 10^{-4}$. Thus the plasma pressure is both indirect and difficult to measure. \vec{B} is the observable of choice since it is strongly divergent and measurable with magnetic probes. We will thus concentrate on the magnetic field measurements.

These experiments employed the Tokapole II device,¹⁴ a noncircular tokamak in a four-node poloidal divertor configuration with a major radius of 50 cm and a square cross-section vacuum chamber 44 cm on a side. The distance from magnetic axis to separatrix is 7–10 cm with parameters of $B_t \leq 8$ kG, $I_p \leq 45$ kA, $T_e \leq 150$ eV, $n_e \leq 10^{13}$ cm⁻³, and pulse length ≤ 12 msec. The divertor currents are driven inductively by the Ohmic heating transformer. To facilitate magnetic probe measurements, the device is derated to $B_t \approx 5$ kG, $T_e \approx 100$ eV, and pulse length ≈ 4 msec, allowing probes to be placed several centimeters inside the separatrix. The safety factor, q , becomes infinite on the divertor separatrix due to x points in the poloidal magnetic field. Since q and the parallel wavelength vary drastically within 2–3 cm of the separatrix, this region can sustain numerous resonances. Stainless-steel limiters are inserted in the divertor scrapeoff region to effectively eliminate plasma current outside the separatrix.

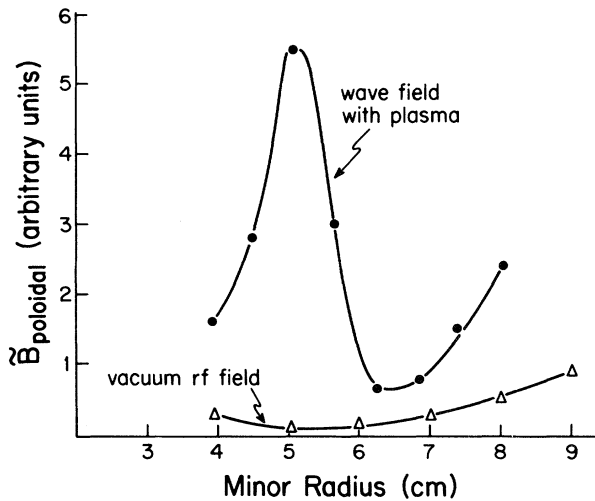


FIG. 1. Poloidal wave magnetic field profile obtained on single shot.

The four solid copper divertor rings are used as the launching structure.⁷ rf currents are superposed on equilibrium currents by grounding one of the three mechanical supports on each ring and driving one of the other supports. Proper phasing of the rf currents in each ring preferentially excites $m=1,2,4$ poloidal mode numbers. The toroidal structure of the antenna currents excites a spectrum of toroidal mode numbers, n , with 75% of the power in the $n=1$ mode. A broad spectrum of m and n modes is thereby generated.

The magnetic probes consist of eight separate five-turn coils of No. 42 Teflon coated wire wound on a dielectric substrate, inserted inside a 0.40-cm-o.d. stainless-steel tube to provide a vacuum seal and electrostatic shield. The coils are spaced along the tube axis to allow a radial profile of \vec{B} to be obtained on a single shot. Toroidal or poloidal field components are measured by rotating the coils inside the tube.

Resonances in the radial profile of the poloidal wave magnetic field are observed as illustrated in one experimental case shown in Fig. 1. The rf field is strongly enhanced above its vacuum value at ~ 5.0 cm from the magnetic axis. In what follows we describe the measured properties of the observed resonances and compare with theoretical predictions.

Resonance location.—The 2D tokamak case was treated both analytically and numerically using ideal MHD.¹³ Analytically, toroidicity is included as a perturbation using the inverse aspect ratio as an expansion parameter. The full equations have been solved numerically for the Tokapole II device.¹³ Expression of the equations in natural flux coordi-

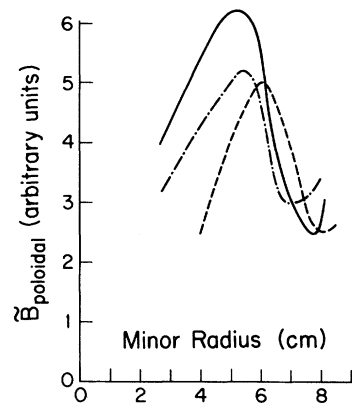


FIG. 2. Radial profile of poloidal wave magnetic field measured along three different chords: $\phi = \theta = 0^\circ$ (solid); $\phi = 30^\circ, \theta = 0^\circ$ (dot-dashed); $\phi = 30^\circ, \theta = 90^\circ$ (dashed). ϕ and θ are toroidal and poloidal azimuths, respectively.

nates reveals that in a tokamak a resonant surface is also a magnetic surface.¹⁵ Experimentally, it does appear that this is so. Figure 2 shows three minor-radius scans of the wave magnetic field; two scans are along horizontal chords at different toroidal locations, and the third scan is a vertical chord. The resonance has a measured symmetry of $|m|=1, |n|=2$. The slight plasma elongation accounts for the dashed curve peaking at a somewhat larger minor radius. Theoretical results for the radial dependence of the resonance frequency are shown in Fig. 3 for the Tokapole II device. At the oscillator frequency of 1.16 MHz the observed resonance

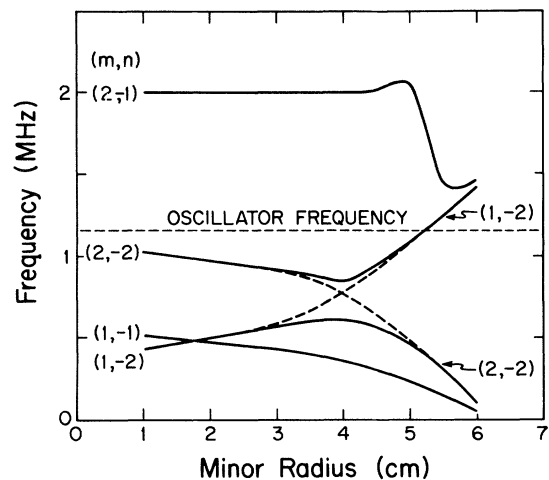


FIG. 3. Resonant frequency vs minor radius as predicted by 2D MHD code (Ref. 13). At drive frequency of 1.16 MHz, theory predicts resonance of $(1,-2)$ mode at 5.0 cm.

is predicted to occur at 5 cm. Of the eight lowest dominant modes, only this mode is predicted to occur near that radius. The modes (3,-1), (4,-1), (3,-2), and (4,-2) all have frequencies that are above 2.5 MHz and are not shown in the figure.

Wave polarization.—Ideal MHD theory for a zero pressure plasma yields the Laplace transform of the wave magnetic field components.¹⁶ At the resonance $\tilde{B}_{\parallel}(\omega)$ is finite, $\tilde{B}_r(\omega) \sim \ln(r-r_0)$ and $\tilde{B}_{\perp}(\omega) \sim (r-r_0)^{-1}$ where \parallel , r , and \perp refer to components parallel to the equilibrium magnetic field, the radial direction, and perpendicular to the equilibrium field within a magnetic surface. $r_0(\omega)$ is the radius resonant at frequency ω . Inverting the transforms yield $\tilde{B}_{\parallel}(t) \sim \sin\omega_0 t$, $\tilde{B}_r \sim \ln t \sin\omega_0 t$ and $\tilde{B}_{\perp} \sim t \sin\omega_0 t$ at the resonant radius with the driving frequency ω_0 . Thus at the resonance, \tilde{B}_{\parallel} remains finite as expected for shear wave resonance, and \tilde{B}_{\perp} is more strongly divergent in time than \tilde{B}_r . After many wave periods the wave magnetic field should be mainly perpendicular to the equilibrium field; i.e., the poloidal wave field should exceed the toroidal wave field by a factor of the inverse aspect ratio or $\tilde{B}_t \sim \epsilon \tilde{B}_p$.

Experimentally, the predicted polarization is observed, as indicated in Fig. 4. The measured \tilde{B}_p typically exceeds \tilde{B}_t by a factor of 7-10 on reso-

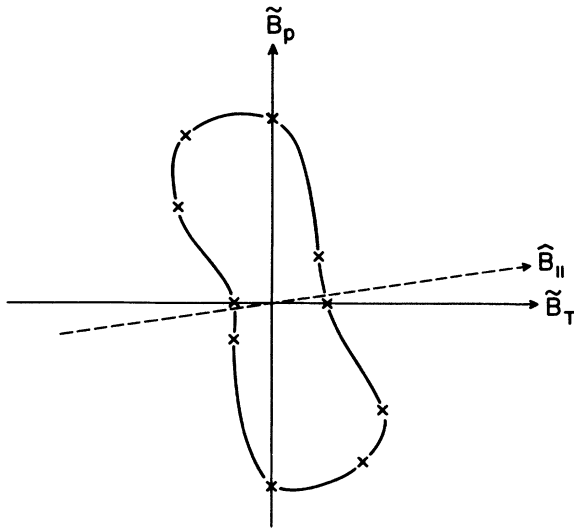


FIG. 4. Polarization plot of measured resonant wave magnetic field, indicating polarization perpendicular to equilibrium field. The distance from the origin to the curve which connects the experimental points (crosses) indicates the magnitude of the wave magnetic field at the corresponding angle. The vertical (horizontal) axis denotes the poloidal (toroidal) direction.

nance, whereas the aspect ratio is 7.

Radial width.—Ideal MHD predicts that as time $t \rightarrow \infty$ the field blows up, and the resonance width, Δ , approaches zero. Dissipation of the wave field will keep \tilde{B} and Δ finite. A resistive MHD boundary layer calculation was performed in Ref. 16 in which resistivity η and Ohmic dissipation was included in a thin layer about the resonant location. The estimated width is given by $\Delta = 8\pi(\eta\rho/\mu_0\omega_0\rho')^{1/3}$. For Tokapole II, this expression yields $\Delta \approx 4-8$ cm. Employing, in the above expression, effective resistivities inferred from the power absorption formulas of Hasegawa and Chen¹⁷ yields the heuristic results that the width due to ion viscosity alone is less than 1 cm and that due to electron Landau damping is about 16 cm. Since the measured widths are roughly 2-5 cm, Ohmic dissipation seems the more likely mechanism. Tokapole II operates with electrons in the plateau collisionality regime.

Rise time.—Ideal MHD predicts that after sudden turn on of a generator the wave fields will grow linearly with time indefinitely. If absorption is included the field should initially rise linearly, and later saturate as the flow of energy to the resonance is balanced by absorption by the plasma. Reference 16 predicts that the rise time to this saturated level is $\tau = (24\mu_0/\omega^2\eta)^{1/3}(\rho/\rho')^{2/3}$. For Tokapole II, the predicted rise time is $\sim 4-9$ μsec . Experimentally, τ has an upper bound of ~ 40 μsec , limited by the oscillator rise time. The observed value is consistent with theory. The enhancement of the resonance wave fields above the vacuum rf fields at saturation calculated from Ref. 17 yields for Tokapole II parameters a value in the range 30-50. Measured enhancement factors are 20-50.

The observed wave enhancement cannot be explained by other well-known low-frequency effects. Since the wave frequency is 100 times larger than the drift wave frequency ($\omega^* \sim 10$ kHz), the mode is not likely a drift wave or unstable resistive or ideal MHD mode, all of which oscillate at $\sim \omega^*$. Since the wave frequency is much lower than the ion cyclotron frequency, finite ω/ω_{ci} effects should not be significant. Since the mode is radially localized, it is not likely a driven stable discrete global kink mode as observed on Pretext¹⁸ and inferred on TCA.¹⁹

In summary, detailed observations have been made of the spatial and temporal structure of the wave magnetic field. Since measurements of the resonance properties such as radial location, wave polarization, resonance width, rise time, and resonant enhancement are all in agreement with

shear Alfvén theory, we believe these observations constitute an identification of the shear Alfvén resonance in a tokamak.

For high-power heating ($P_{\text{rf}} \sim 1$ MW) experiments, four separate Faraday shielded antennas²⁰ are being installed which will be radially movable and rotatable so as to determine the optimal antenna orientation. Each antenna is a double-turn loop. One of these antennas has already been installed and a resonance observed 90° away toroidally from the antenna.

The authors are grateful to C. Kieras and J. Tataronis for developing the numerical code for calculating resonance locations in Tokapole II and for numerous helpful discussions, to D. Kortbawi for extensive aid with equipment and data taking, to T. Osborne and N. Brickhouse for help with the equilibrium code, and to T. Lovell for his invaluable engineering support.

This work was supported by the U.S. Department of Energy.

¹E. M. Barston, *Ann. Phys. (N.Y.)* **29**, 282 (1964).

²C. Uberoi, *Phys. Fluids* **15**, 1673 (1972).

³W. Grossmann and J. Tataronis, *Z. Phys.* **261**, 203 and 217 (1973).

⁴A. Hasegawa and L. Chen, *Phys. Rev. Lett.* **32**, 454 (1974), and *Phys. Fluids* **17**, 1399 (1974).

⁵A. DeChambrier *et al.*, *Plasma Phys.* **24**, 893 (1982); R. Keller *et al.*, in *Proceedings of the Fourth Topical Conference on rf Plasma Heating, Austin, Texas, 1981*, edited by R. D. Bengtson and M. E. Oakes (Univ. of Texas Press, Austin, 1981).

⁶D. W. Ross *et al.*, in *Proceedings of the Fourth Topical Conference on rf Plasma Heating, Austin, Texas, 1981*, edited by R. D. Bengtson and M. E. Oakes (Univ. of Texas, Austin, 1981).

⁷F. D. Witherspoon *et al.*, in *Proceedings of the Fourth Topical Conference on rf Plasma Heating, Austin, Texas, 1981*, edited by R. D. Bengtson and M. E. Oakes (Univ. of Texas Press, Austin, 1981); see also, S. C. Prager *et al.*, in *Proceedings of the Fifth Topical Conference on Radio Frequency Plasma Heating, University of Wisconsin, Madison, Wisconsin, 1983* (to be published).

⁸R. C. Cross *et al.*, in *Heating in Toroidal Plasmas III*, edited by C. Gormezano (Pergamon, New York, 1982) Vol. 1, p. 183.

⁹R. A. Demirkhanov *et al.*, in *Proceedings of the Ninth International Conference on Plasma Physics and Controlled Nuclear Fusion Research, Baltimore, 1-8 September 1982* (International Atomic Energy Agency, Vienna, 1983).

¹⁰R. Keller and A. Pochelon, *Nucl. Fusion* **18**, 1051 (1978).

¹¹S. N. Golovato and J. L. Shohet, *Phys. Fluids* **21**, 1421 (1978); K. Uo *et al.*, in *Proceedings of the Sixth International Conference on Plasma Physics and Controlled Nuclear Fusion Research, Berchtesgaden, West Germany, 1976* (International Atomic Energy Agency, Vienna, 1977).

¹²A. Tsushima, Y. Amagishi, and M. Inutake, *Phys. Lett.* **88A**, 457 (1981).

¹³C. E. Kieras and J. A. Tataronis, *J. Plasma Phys.* **28**, 395 (1982).

¹⁴A. P. Biddle *et al.*, *Nucl. Fusion* **9**, 1509 (1979).

¹⁵J. A. Tataronis, J. N. Talmadge, J. L. Shohet, in *Proceedings of the Third Topical Conference on rf Plasma Heating, Pasadena, California, 1978*, edited by R. Gould (Caltech, Pasadena, 1978).

¹⁶J. M. Kappraff and J. A. Tataronis, *J. Plasma Phys.* **18**, 209 (1979).

¹⁷A. Hasegawa and L. Chen, *Phys. Fluids* **19**, 1924 (1976).

¹⁸R. D. Bengtson *et al.*, in *Proceedings of the Fifth Topical Conference on Radio Frequency Plasma Heating, University of Wisconsin, Madison, Wisconsin, 1983* (to be published).

¹⁹K. Appert, R. Gruber, F. Troyon, and J. Vaclavik, *Plasma Physics* **24**, 1147 (1982).

²⁰D. Kortbawi, F. D. Witherspoon, J. C. Sprott, and S. C. Prager, *Bull. Am. Phys. Soc.* **28**, 1086 (1983).